# Supplementary Figures

Supplementary Figure 1

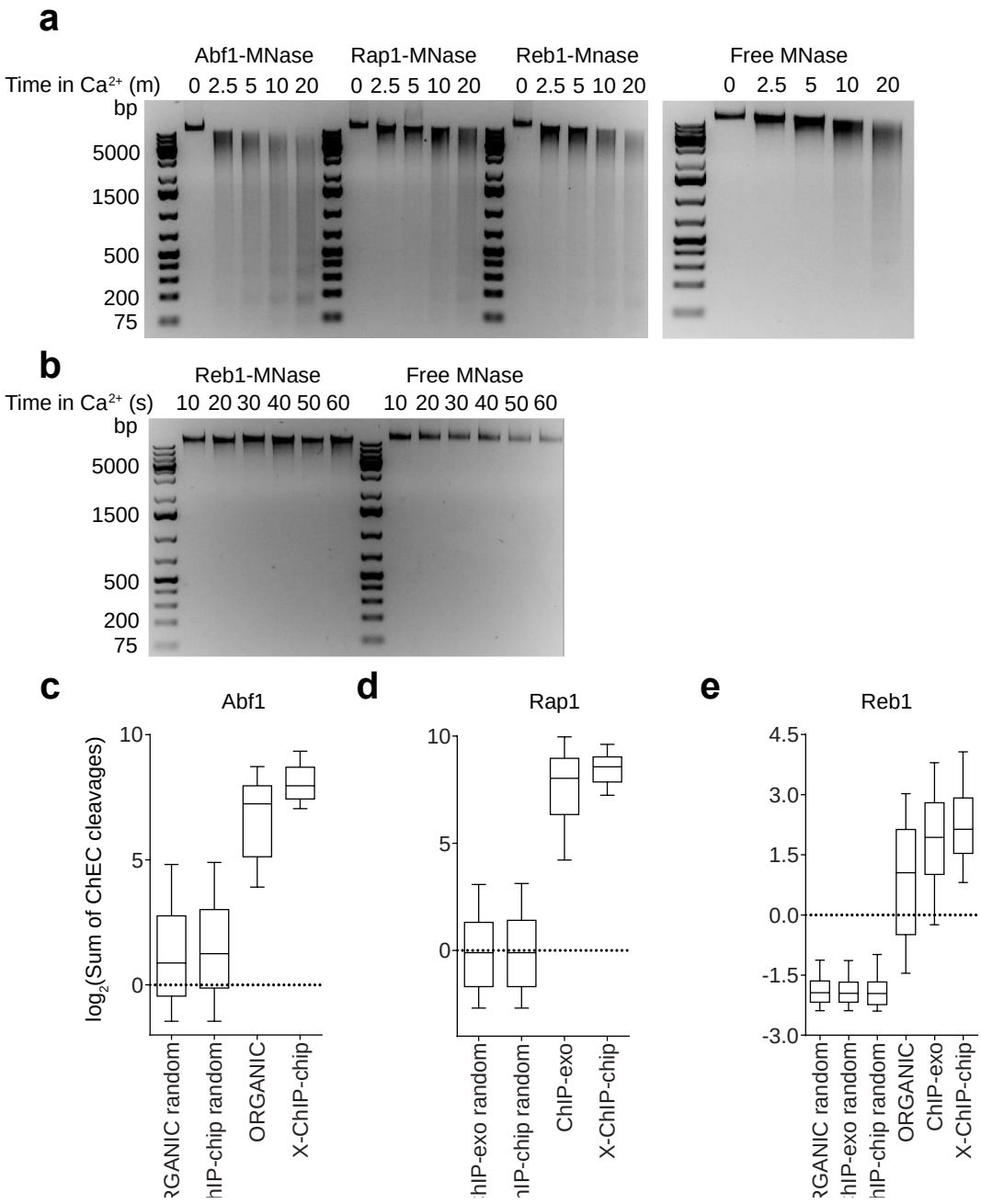


**Supplementary Figure 1. Specificity of ChEC-seq**

(**a**) Agarose gel analysis of genomic DNA from TF-MNase and free MNase strains 0, 2.5, 5, 10, and 20 m after calcium addition. (**b**) Agarose gel analysis of genomic DNA from Reb1-MNase and free MNase strains 10, 20, 30, 40, 50, and 60 s after calcium addition. Also shown are boxplots of total ChEC-seq cleavages at peaks previously determined by various ChIP methods and an equal number of random sites for (**c**) Abf1, (**d**) Rap1, and (**e**) Reb1.

Supplementary Figure 2

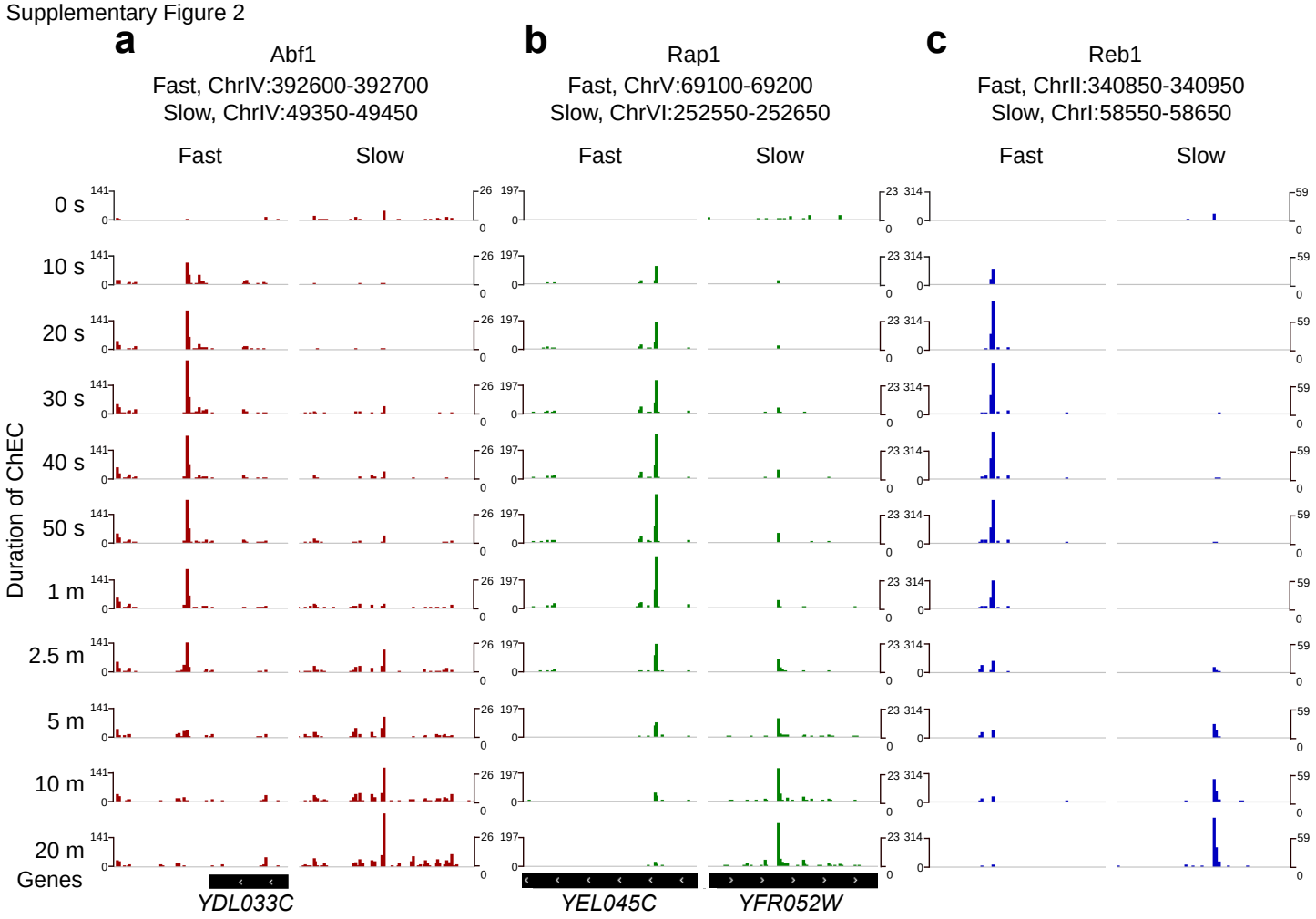


**Supplementary Figure 2. Fast and slow ChEC-seq sites**

Tracks of ChEC-seq signal at a fast and slow site for (**a**) Abf1, (**b**) Rap1, and (**c**) Reb1.

Supplementary Figure 3

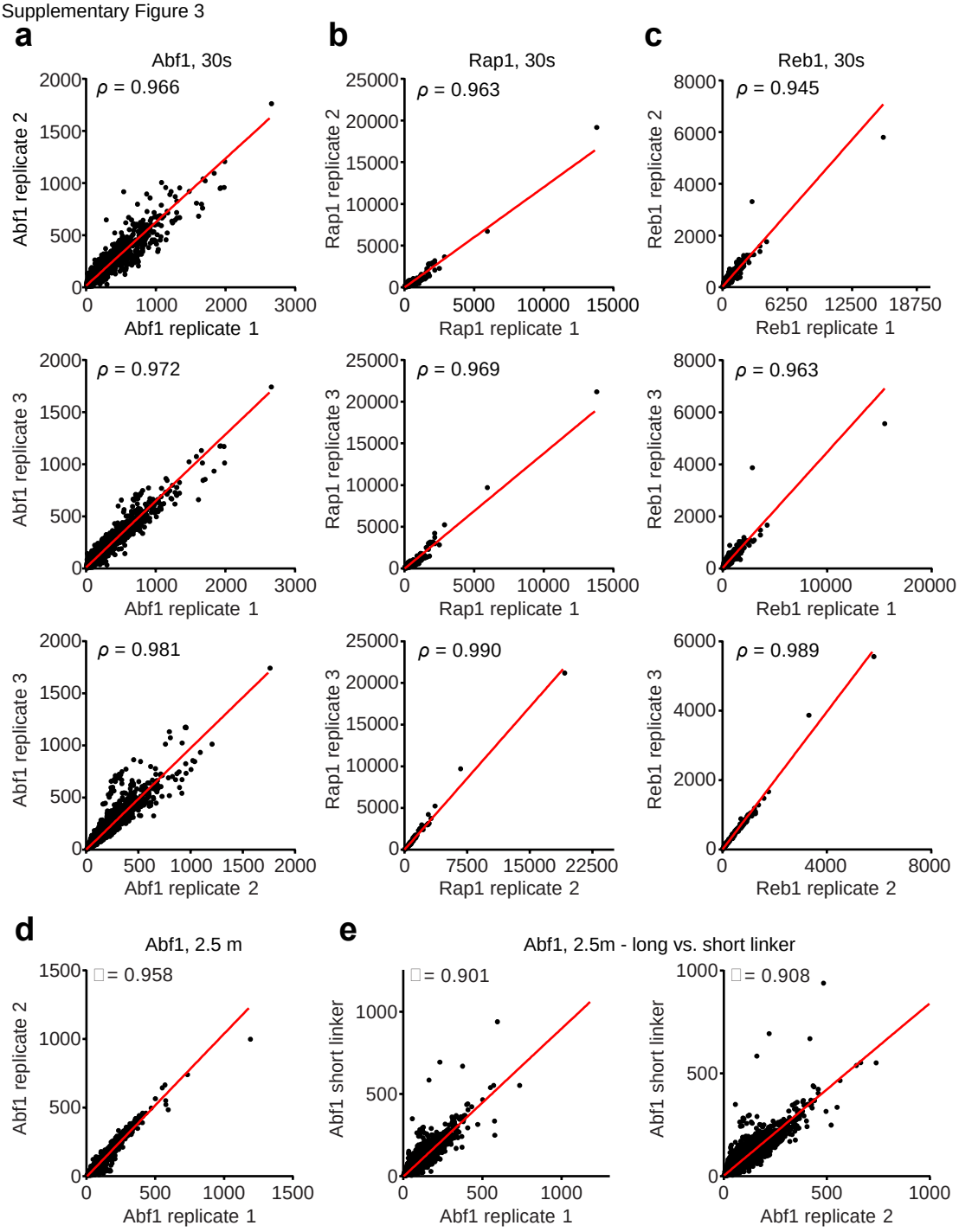


**Supplementary Figure 3. ChEC-seq peaks are highly reproducible**

Pairwise correlations of 30 s ChEC-seq replicate signal at (**a**) Abf1, (**b**) Rap1, and (**c**) Reb1 peaks. (**d**) Pairwise correlation of 2.5 m ChEC-seq replicate signal. (**e**) Pairwise correlations of 2.5 m Abf1 ChEC-seq replicate signal with 2.5 m Abf1 short linker ChEC-seq signal. The sum of cleavages in a 50 bp window around each peak midpoint was taken to be that peak's occupancy. The Spearman's rank correlation coefficient $\rho$ for each pairwise comparison is reported.

Supplementary Figure 4

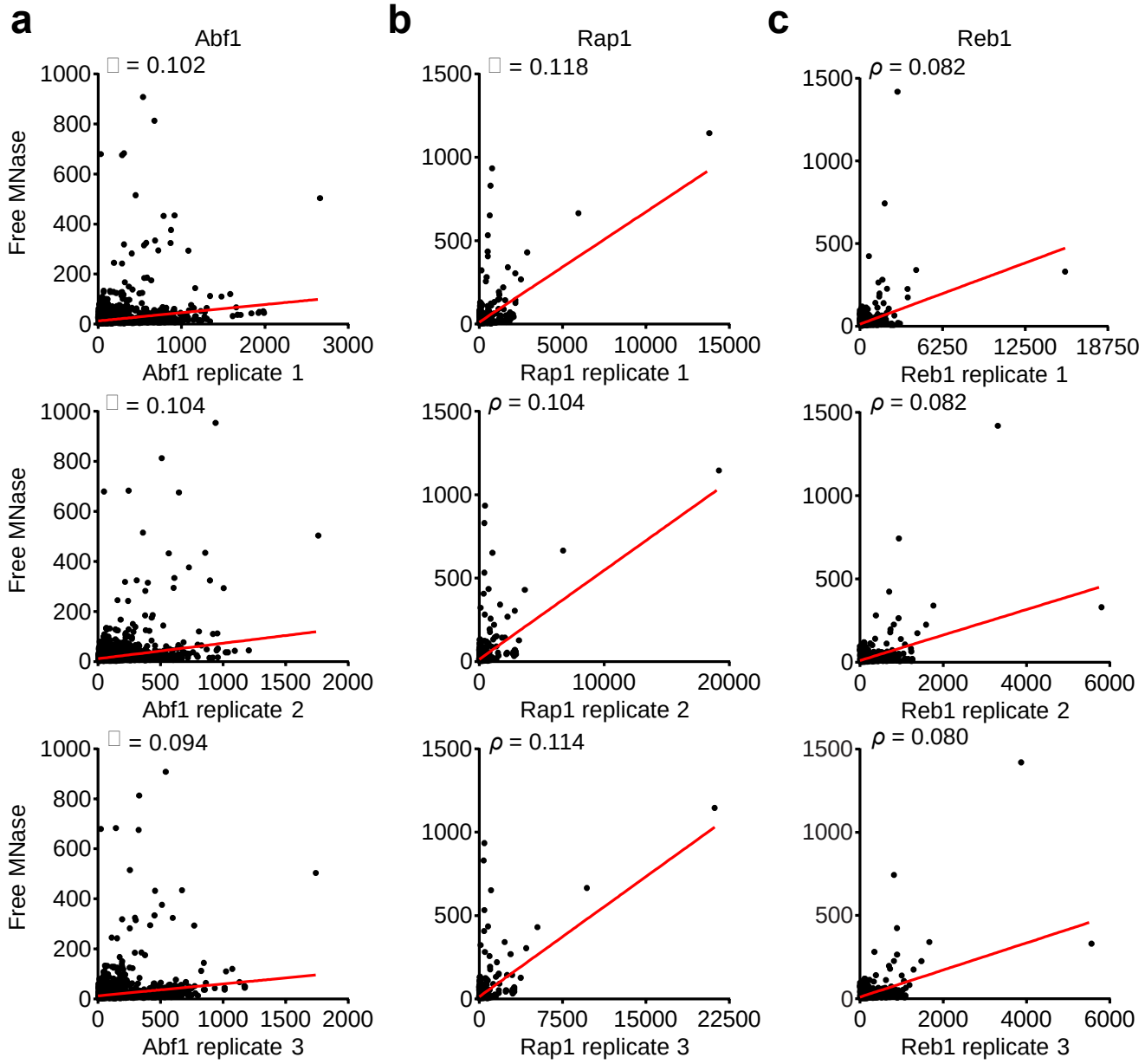


**Supplementary Figure 4. ChEC-seq peaks show poor correlation with free MNase signal**

Pairwise correlations of 30 s ChEC-seq and free MNase signal at (**a**) Abf1, (**b**) Rap1, and (**c**) Reb1 peaks. The sum of cleavages in a 50 bp window around each peak midpoint was taken to be that peak's occupancy. The Spearman's rank correlation coefficient $\rho$ for each pairwise comparison is reported.

Supplementary Figure 5

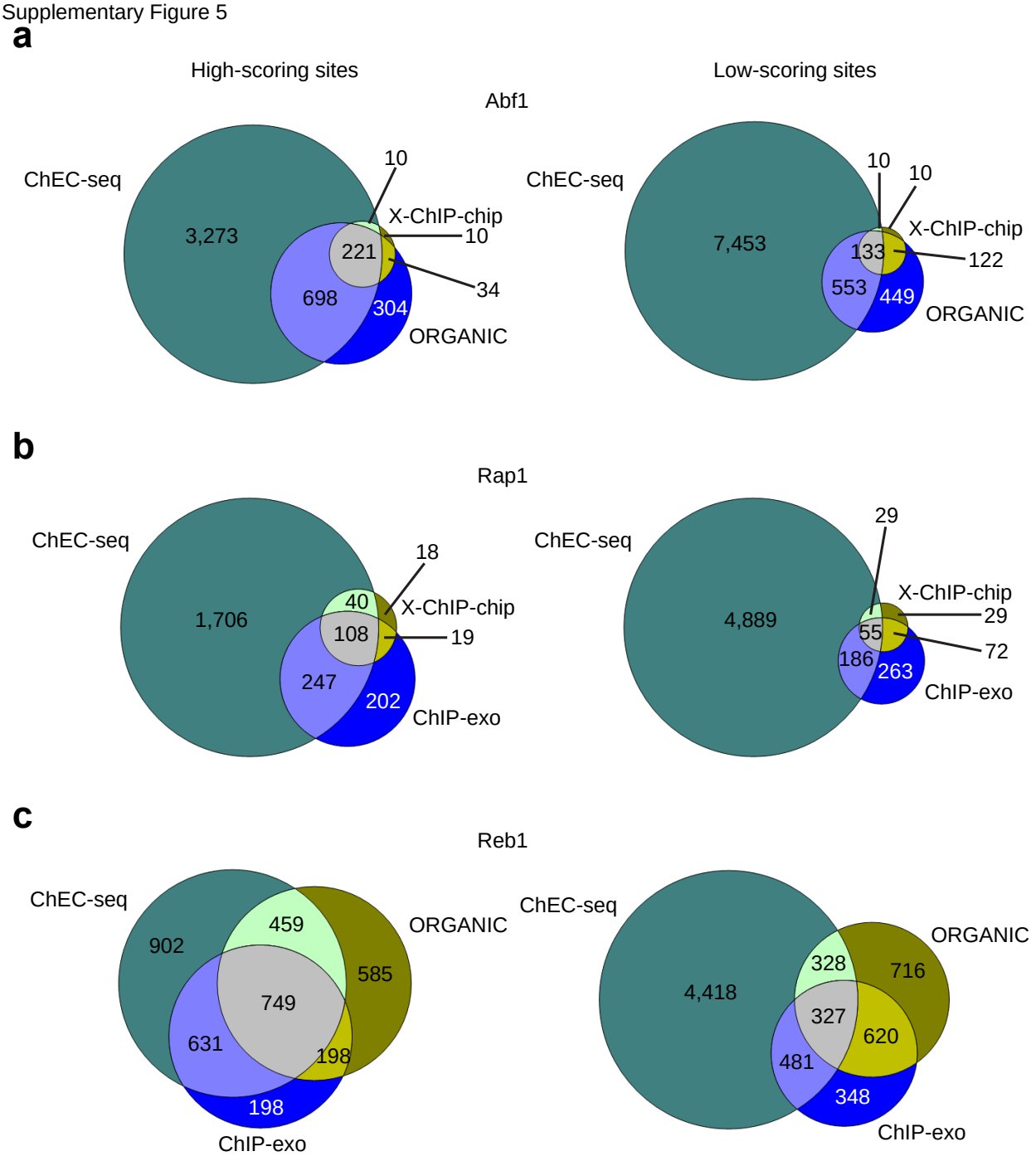


**Supplementary Figure 5. Overlap of ChEC-seq peaks with ChIP peaks**

(**a**) Venn diagrams of overlap between high- and low-scoring Abf1 ChEC-seq sites with Abf1 X-ChIP-chip and ORGANIC peaks. (**b**) Venn diagrams of overlap between high- and low-scoring Rap1 ChEC-seq sites with Rap1 X-ChIP-chip and ChIP-exo peaks. (**c**) Venn diagrams of overlap between high- and low-scoring Reb1 ChEC-seq sites with Reb1 ORGANIC and ChIP-exo peaks.

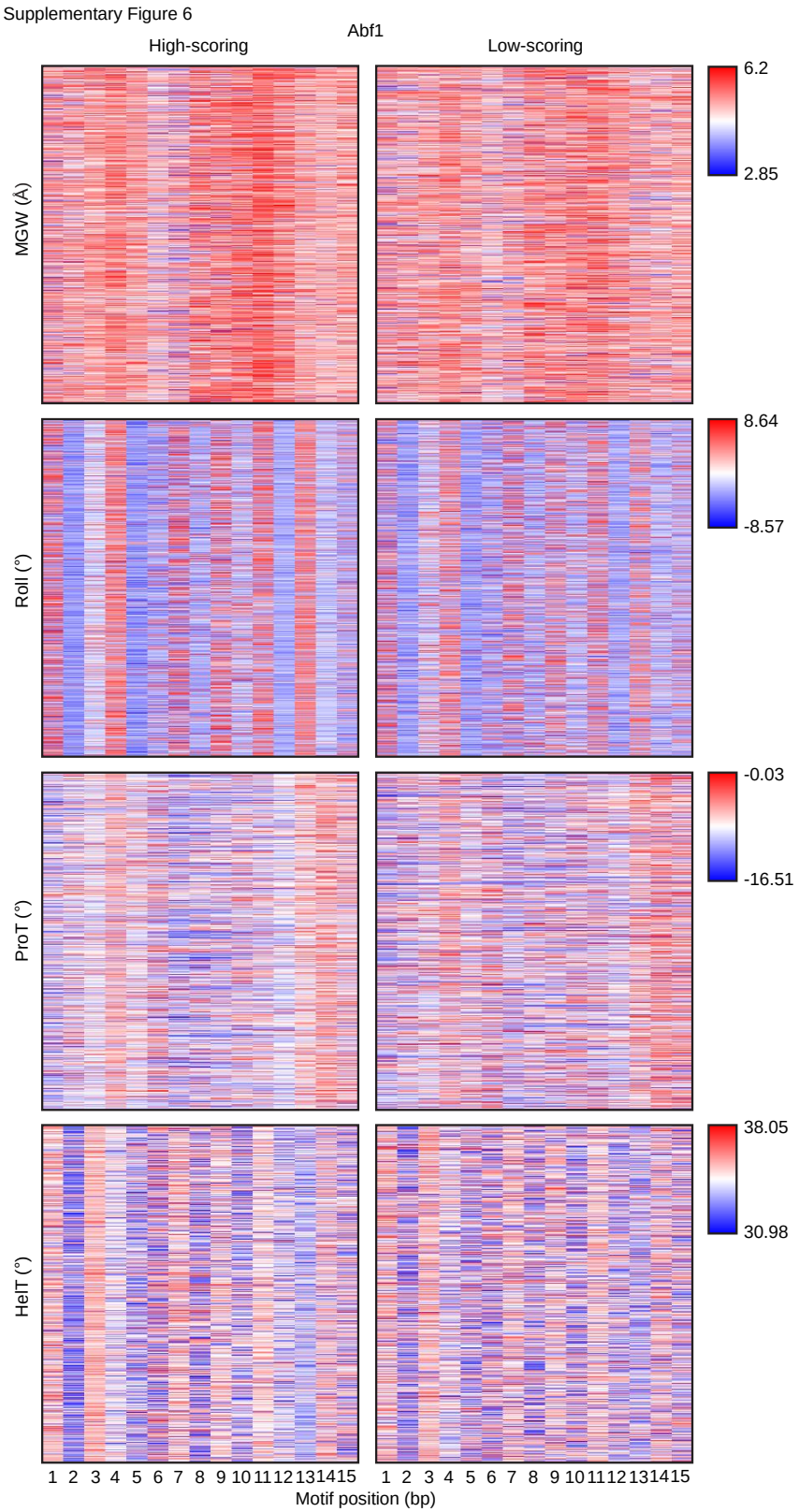


**Supplementary Figure 6. High-scoring and low-scoring Abf1 sites display similar shape profiles.** Heatmaps of DNA shape features minor groove width (MGW), Roll, propeller twist (ProT), and helix twist (HelT) around high- and low-scoring Abf1 sites ranked ascending by motif match *p*-values.

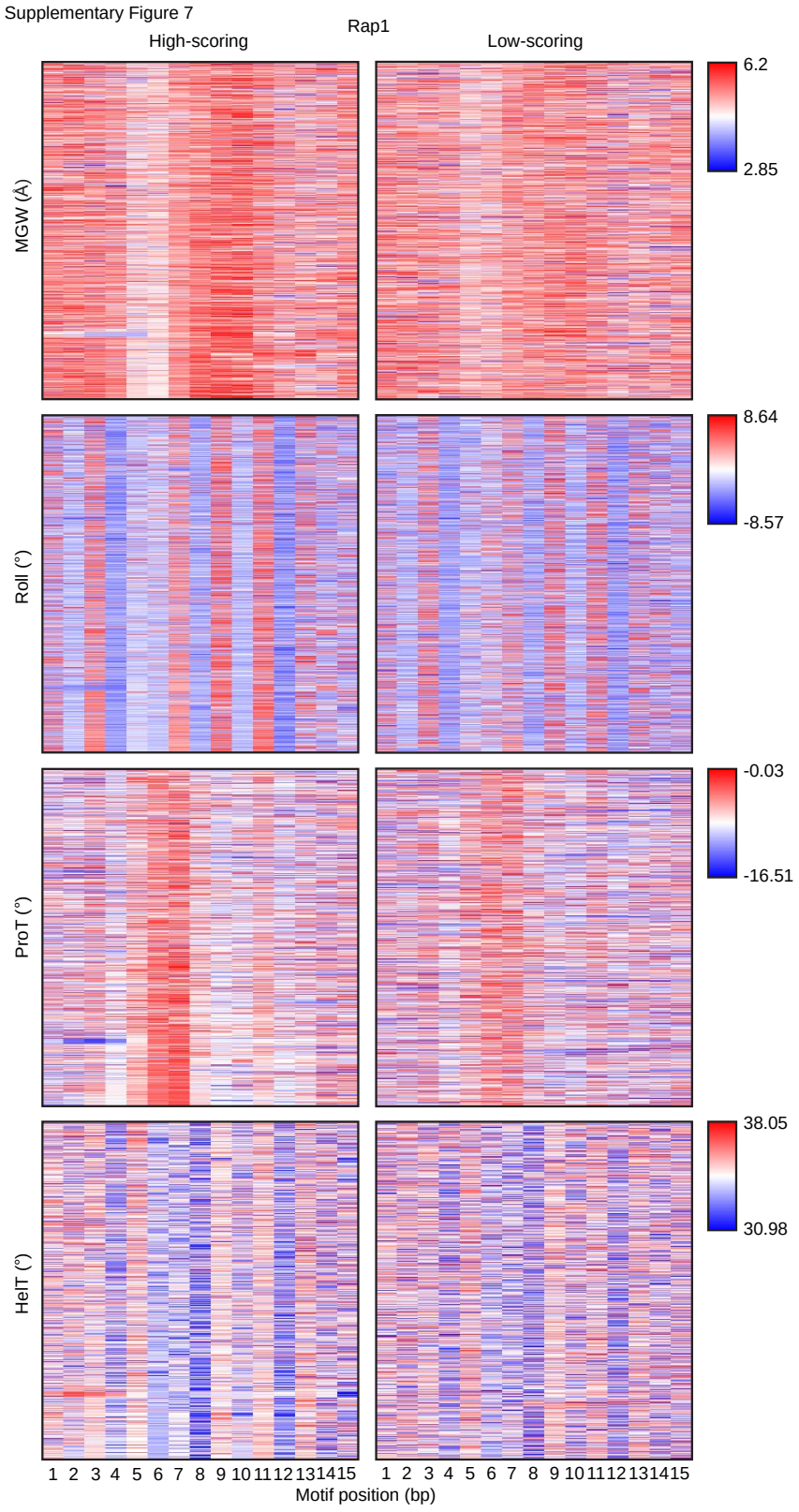


**Supplementary Figure 7. High-scoring and low-scoring Rap1 sites display similar shape profiles.** Heat maps of DNA shape features minor groove width (MGW), Roll, propeller twist (ProT), and helix twist (HelT) around high- and low-scoring Rap1 sites ranked ascending by motif match *p*-values.

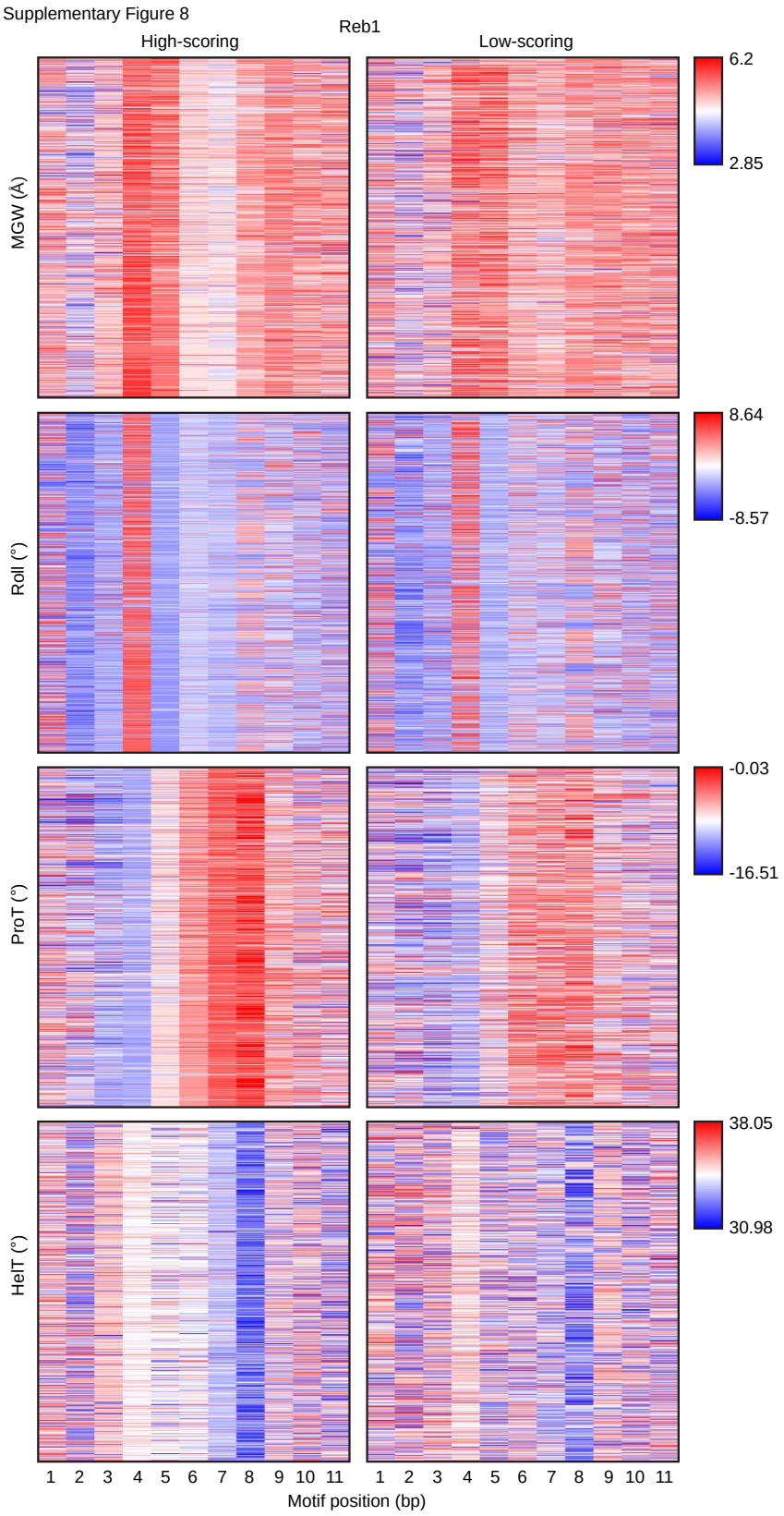


**Supplementary Figure 8. High-scoring and low-scoring Reb1 sites display similar shape profiles.** Heat maps of DNA shape features minor groove width (MGW), Roll, propeller twist (ProT), and helix twist (HelT) around high- and low-scoring Reb1 sites ranked ascending by motif match *p*-values.

Supplementary Figure 9

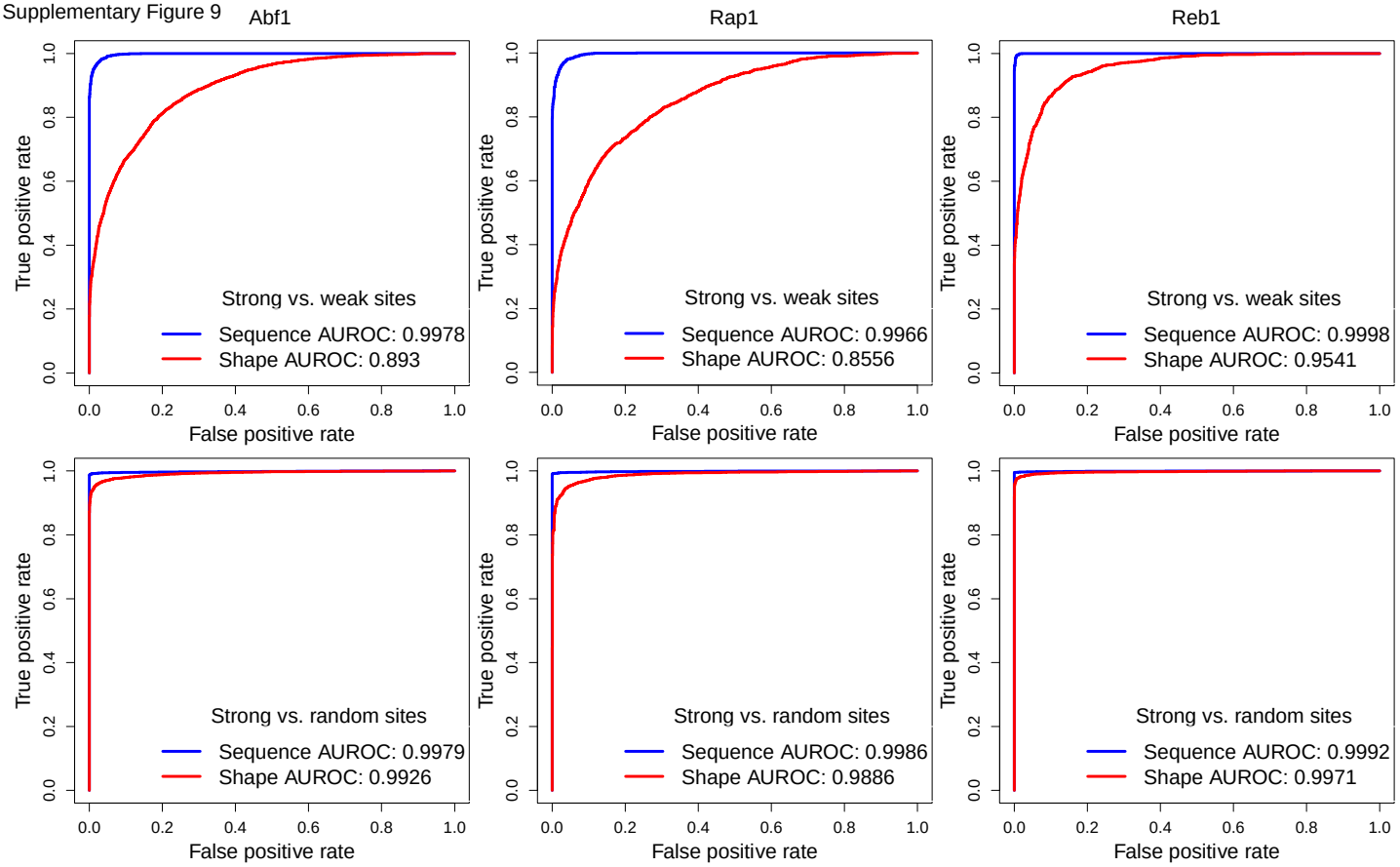


**Supplementary Figure 9. Classification of high-scoring and low-scoring motif sites using DNA sequence or shape.** Models based on L2-regularized multiple linear regression (MLR) encoding either sequence (blue) or shape (red) were used to distinguish sequences containing high-scoring and low-scoring motifs (top row) for Abf1 (left), Rap1 (center), and Reb1 (right). The lower AUROC values for the shape-based classification indicate the higher similarity of high-scoring and low-scoring sites in terms of DNA shape compared to sequence. This difference between sequence- and shape-based models cannot be observed when the MLR classification is applied to sequences containing high-scoring motifs and random sequences (bottom row).

## Supplementary Tables

| Plasmid | Description | Source |
|---|---|---|
| pFA6a-3HA-KanMX6 | C-terminal 3xHA-tagging vector (F2/R1 compatible), kanMX6 | Addgene |
| pFA6a-3HA-HIS3MX6 | C-terminal 3xHA-tagging vector (F2/R1 compatible), HIS3MX6 | Addgene |
| pFA6a-3HA-TRP1 | C-terminal 3xHA-tagging vector (F2/R1 compatible), TRP1 | Addgene |
| pFA6a-kanMX6 | Deletion vector (F2/R1 compatible), kanMX6 | Sue Biggins |
| pGZ108 | C-terminal 3xFLAG-MNase-tagging vector (F2/R1 compatible), kanMX6 | This study |
| pGZ109 | C-terminal 3xFLAG-MNase-tagging vector (F2/R1 compatible), HIS3MX6 | This study |
| pGZ110 | C-terminal 3xFLAG-MNase-tagging vector (F2/R1 compatible), TRP1 | This study |
| pGZ136 | 3xFLAG-MNase-SV40 NLS under the control of the *REB1* promoter in pRS406 | This study |
| pGZ172 | MNase-3FLAG-REB1 under the control of the *REB1* promoter in pRS413 | This study |
| pGZ173 | C-terminal short linker-MNase-tagging vector (F2/R1 compatible), kanMX6 | This study |
| pRS406 | Integrating vector, URA3 | Toshio Tsukiyama |
| pRS413 | Shuttle vector, HIS3 | Toshio Tsukiyama |

**Supplementary Table 1. Plasmids used in this study**

| Strain | Genotype | Source |
|---|---|---|
| GZY85 | *MATa ade2-1 can1-100 his3-11, 15 leu2-3, 112 trp1-1 ura3-1 RAD5+ REB1-3FLAG-MNase-kanMX6* | This study |
| GZY98 | *MATa ade2-1 can1-100 his3-11, 15 leu2-3, 112 trp1-1 ura3-1 RAD5+ ura3::$P_{REB1}$-3FLAG-MNase-URA3* | This study |
| GZY99 | *MATa ade2-1 can1-100 his3-11, 15 leu2-3, 112 trp1-1 ura3-1 RAD5+ ABF1-3FLAG-MNase-kanMX6* | This study |
| GZY100 | *MATa ade2-1 can1-100 his3-11, 15 leu2-3, 112 trp1-1 ura3-1 RAD5+ RAP1-3FLAG-MNase-kanMX6* | This study |
| GZY112 | *MATa ade2-1 can1-100 his3-11, 15 leu2-3, 112 trp1-1 ura3-1 RAD5+ ABF1-SL-MNase-kanMX6* | This study |
| GZY113 | *MATa ade2-1 can1-100 his3-11, 15 leu2-3, 112 trp1-1 ura3-1 RAD5+ RAP1-SL-MNase-kanMX6* | This study |
| GZY114 | *MATa ade2-1 can1-100 his3-11, 15 leu2-3, 112 trp1-1 ura3-1 RAD5+ REB1-SL-MNase-kanMX6* | This study |
| GZY115 | *MATa ade2-1 can1-100 his3-11, 15 leu2-3, 112 trp1-1 ura3-1 RAD5+ reb1$\Delta$::kanMX6 pGZ172 ($P_{REB1}$-MNase-3FLAG-REB1 HIS3 CEN ARS)* | This study |
| SKY1 | *MATa ade2-1 can1-100 his3-11, 15 leu2-3, 112 trp1-1 ura3-1 RAD5+ ABF1-3FLAG-kanMX4* | Kasinathan *et al*.[1] |

**Supplementary Table 2. Yeast strains used in this study**
All strains were constructed in the W1588-4C background, which is isogenic to W303-1A except that a weak *rad5* mutation is repaired[2].

## Supplementary References


1. Kasinathan, S., Orsi, G.A., Zentner, G.E., Ahmad, K. & Henikoff, S. High-resolution mapping of transcription factor binding sites on native chromatin. *Nat Meth* **11**, 203-209 (2014).
2. Zhao, X., Muller, E.G.D. & Rothstein, R. A Suppressor of Two Essential Checkpoint Genes Identifies a Novel Protein that Negatively Affects dNTP Pools. *Mol Cell* **2**, 329-340 (1998).